RSC Advances

Single-LED solar simulator for amorphous Si and dye-sensitized solar cells

SCHOLARONE™
Manuscripts

Journal Name

ARTICLE

Single-LED solar simulator for amorphous Si and dye-sensitized solar cells

Tomohiko Nakajima,[*] Kentaro Shinoda and Tetsuo Tsuchiya

An optimal combination of phosphors that simulates the solar spectrum under excitation at 365 nm has been revealed. $CsVO_3$ and $Zn_3V_2O_8$ vanadate phosphors that have broadband luminescence, Eu^{2+}/Mn^{2+}-doped silicates and aluminosilicates, and Fe^{2+}-doped Li gallate were investigated as luminescence sources. The mixed phosphor powders had an internal quantum efficiency of 29.2%, a high color rendering index of 99, and a correlated color temperature of 5645 K. We fabricated a prototype LED solar simulator consisting of the optimized phosphor powder mixture embedded in resin on a silica glass substrate, and one high-power UV light-emitting diode (LED) with an emission wavelength of 365 nm. Our simulator achieved a Class A spectral match with the AM1.5G solar spectrum in the JIS C 8933 standard. An irradiance of 100 mW·cm^{-2} was measured at a forward driving current of 700 mA for the UV LED. This system functioned well as a solar simulator for solar cell testing. The *I-V* curves of a Si photodiode calibrated as an amorphous Si solar cell and of a TiO_2 dye-sensitized solar cell were very similar to the *I-V* curves measured under a conventional Xe lamp solar simulator.

Introduction

Solar energy is an essential power source, providing energy for everything from plants to photovoltaics. Solar cells,[1–4] solar thermal systems,[5–7] photocatalysts,[8–11] and plant factories[12–14] have all been extensively investigated. Light sources that reproduce the solar spectrum and power, known as solar simulators, are vital for testing solar devices.[15–17] The standard solar spectrum and irradiance are defined as air mass (AM) 1.5G,[18,19] which has an irradiance of 100 mW·cm^{-2} (1 SUN). Moreover, official standards have been established specifically by the International Electrotechnical Commission (IEC), the Japanese Industrial Standards (JIS) Committee, and the Optoelectronic Industry and Technology Development Association (OITDA) for testing solar cells in two main wavelength ranges. The range for polycrystalline Si solar cells is 400–1100 nm (IEC 60904-9[20] and JIS C 8912[21]), and that for amorphous Si and dye-sensitized solar cells 350–750 nm (JIS C 8933[22] and OITDA-PV01[23]). Solar simulators have been developed based on these official standards. Currently, Xe lamps (150–500 W) equipped with an AM1.5G filter are usually used as the light source in solar simulators.[16,19,24] Due to recent growth of solar cell research, however, the energy efficiency of research activities themselves has recently become a concern. Thus, a new type of solar simulator using multicolor light-emitting diodes (LEDs) has been developed.[25–30] LEDs extend the working life of solar simulators considerably,

compared with Xe lamp sources (Fig. 1). However, LED simulators use a large number of LEDs of many different types to provide uniform coverage of the sunlight spectrum. Therefore, a simpler method for simulating the sunlight spectrum with LEDs is still required.

We have studied the luminescence properties of vanadate phosphors, and showed that they have an intense emission and very broad spectral range for ultraviolet (UV) excitation below 400 nm.[31–35] In particular, $CsVO_3$ and $Zn_3V_2O_8$ showed broadband luminescence over a range of 400–800 nm with emission peaks at 525 and 575 nm.[33,34] The emission efficiency of UV LEDs has also improved substantially;[36,37] the optical power of a commercial UV LED (NC4U133A, Nichia) emitting at 365 nm is 1950 mW at a driving current of 500 mA. Aiming to build on these recent advances, we set out to make an efficient solar simulator for amorphous Si and dye-sensitized solar cells using just a single LED chip and UV-active phosphors (Fig. 1), because we expected that the broadband luminescence of $CsVO_3$ and $Zn_3V_2O_8$ was highly-promising to simulate the solar spectrum well.
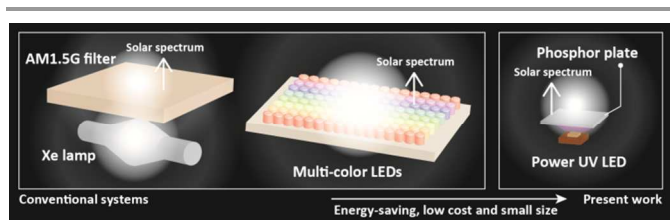
Fig. 1. Schematic of a conventional solar simulator and our solar simulator.

Experimental procedure

To produce the sunlight spectra, we selected 10 UV-active phosphors with broadband luminescence. We used vanadate phosphors ($CsVO_3$ and $Zn_3V_2O_8$) for visible light emission, Eu^{2+}/Mn^{2+}-doped silicates[38–40] and aluminosilicates[41] for UV and visible light emission, and Fe^{2+}-doped gallate[42] for near-infrared emission. Polycrystalline phosphor powders were synthesized by solid-state reactions using previously reported procedures (Table S1†).[38–42] The purity and crystallinity of the polycrystalline samples were confirmed by X-ray powder diffraction. All polycrystalline samples consisted of a well-crystallized single phase with no impurities (Fig. S1†). The particle shape of obtained samples was granular with the size from a few microns to 50 micron meter (Fig. S2†). The photoluminescence (PL) and excitation (PLE) spectra, the internal quantum efficiency (IQE) values, and the luminescent color properties of the samples were evaluated with a spectrometer (C9920-02, Hamamatsu Photonics) equipped with a 150 W Xe lamp as the excitation light source, a monochromator, a high-sensitivity back-illuminated multi-channel charge-coupled device (CCD) photodetector, and an integrating sphere. The CCD photodetector used in this study had a higher reliability for measuring long-wavelength emissions ($\lambda > 700$ nm) compared with the photomultiplier tubes in commercial spectrofluorometers. IQE (%) was calculated as IQE = $N_{em}/N_{abs} \times 100$, where N_{abs} and N_{em} are the number of absorbed and emitted photons, respectively.

A single-LED solar simulator was assembled from a high-power UV LED with an emission wavelength of 365 nm (NC4U133A, Nichia) and a phosphor plate that was prepared by depositing a mixture of phosphor powders embedded in silicone resin on a 0.5-mm-thick silica glass substrate. The phosphor plate was placed several millimeters above the UV LED chip on thermally insulating supports. The irradiance of the prepared LED solar simulator was measured by a Si photodiode detector (BS-520BK, Bunkoukeiki) calibrated with a standardized light source. For comparison, we also used a conventional Xe lamp solar simulator (10500, ABET Technologies) that has a class A spectral match for the IEC and JIS standards. The *J-V* curves were obtained under 1 SUN illumination by using a Si photodetector with a color correction filter (BPW21R, Vishay) to mimic an amorphous Si solar cell, and a dye-sensitized solar cell that was prepared by a conventional procedure for commercial Grätzel cells consisting of a porous TiO_2 layer, a Ru-based dye (di-tetrabutylammonium *cis*-bis(isothiocyanato)bis(2,2-bipyridyl-

4,4'-dicarboxylato)ruthenium (II); N719, Solaronix), and an electrolyte (Z-50, Solaronix).[4,43]

Results and discussion

Luminescence properties of prepared phosphors

First, we prepared the vanadate phosphors $CsVO_3$ and $Zn_3V_2O_8$, and confirmed that their luminescence spectra covered a wide range of visible light wavelengths in the sunlight spectrum (AM1.5G). Full width at half maximum (FWHM) values of 170 and 200 nm were observed for $CsVO_3$ and $Zn_3V_2O_8$, respectively (Fig. 2a). Figures 2b and c show PLE and IQE as a function of wavelength. Both phosphors had a sufficiently high value at 365 nm for the UV LED excitation wavelength; an IQE of 85.0% and 46.2% was recorded for $CsVO_3$ and $Zn_3V_2O_8$, respectively, at 365 nm. To fill the gap between the AM1.5G spectrum and the spectra of the vanadate phosphors in the UV–blue and red regions, we used emissions from Eu^{2+} and Mn^{2+} luminescence color centers, which generally have an emission FWHM of 50–100 nm. We prepared Eu^{2+}/Mn^{2+}-doped silicates ($Ba_{2.91}MgSi_2O_8:Eu_{0.04}Mn_{0.05}$, $Ba_{1.83}Sr_{0.5}Ca_{0.5}MgSi_2O_8:Eu_{0.02}Mn_{0.15}$, $Sr_{2.83}MgSi_2O_8:Eu_{0.02}Mn_{0.15}$, $Ca_{2.83}MgSi_2O_8:Eu_{0.02}Mn_{0.15}$, and $Ba_{0.985}Mg_{1.8}Si_2O_7:Eu_{0.015}Mn_{0.2}$) and aluminosilicates ($Ba_{0.95}Al_2Si_2O_8:Eu_{0.05}$ and $Sr_{0.95}Al_2Si_2O_8:Eu_{0.05}$). For infrared wavelengths, we used an Fe-doped lithium gallate ($LiGaO_2:Fe_{0.01}$) that has broadband emission with a FWHM of 100 nm. The IQE, absorbance, and CIE color coordinates of the phosphors are listed in Table 1.
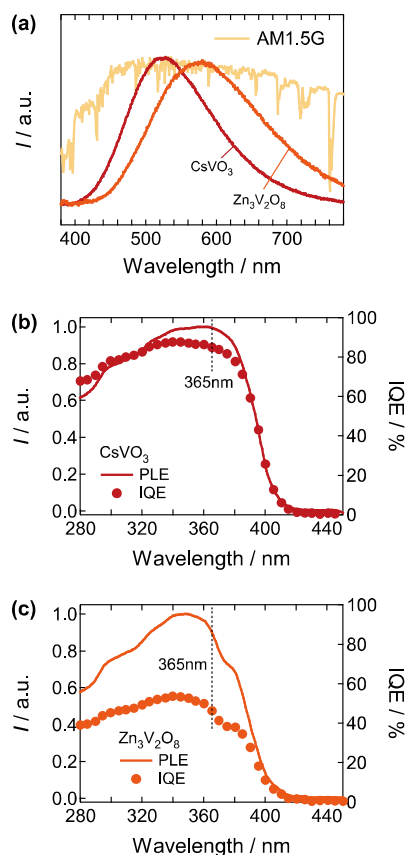
Fig. 2 (a) PL spectra for $CsVO_3$ and $Zn_3V_2O_8$, PLE and IQE spectra of (b) $CsVO_3$ and (c) $Zn_3V_2O_8$.

Table 1. IQE, absorption, CIE coordinate, and weight fraction for the solar phosphor mixture.[a]

Material	IQE / %	Abs. / a.u.[b]	CIE(x,y)	Wt %
$CsVO_3$	85.0	47.5	0.324,0.452	0.543
$Zn_3V_2O_8$	46.2	47.1	0.432,0.475	8.283
$Ba_{2.91}MgSi_2O_8:Eu_{0.04},Mn_{0.05}$	67.4	47.6	0.344,0.146	0.581
$Ba_{1.83}Sr_{0.5}Ca_{0.5}MgSi_2O_8:Eu_{0.02}Mn_{0.15}$	75.8	32.2	0.223,0.090	1.406
$Sr_{2.83}MgSi_2O_8:Eu_{0.02}Mn_{0.15}$	62.0	39.7	0.156,0.070	0.796
$Ca_{2.83}MgSi_2O_8:Eu_{0.02}Mn_{0.15}$	44.2	36.1	0.169,0.273	1.191
$Ba_{0.985}Mg_{1.8}Si_2O_7:Eu_{0.015}Mn_{0.2}$	26.2	31.2	0.484,0.364	11.805
$Ba_{0.95}Al_2Si_2O_8:Eu_{0.05}$	17.1	32.8	0.174,0.162	1.270
$Sr_{0.95}Al_2Si_2O_8:Eu_{0.05}$	46.1	34.6	0.165,0.100	1.962
$LiGaO_2:Fe_{0.01}$	76.7	13.0	0.380,0.231	72.163

[a]Optical data taken under excitation at 365 nm. [b]Absorbance evaluated by comparison of photon numbers of the incident and reflection light for each 0.02 g sample.
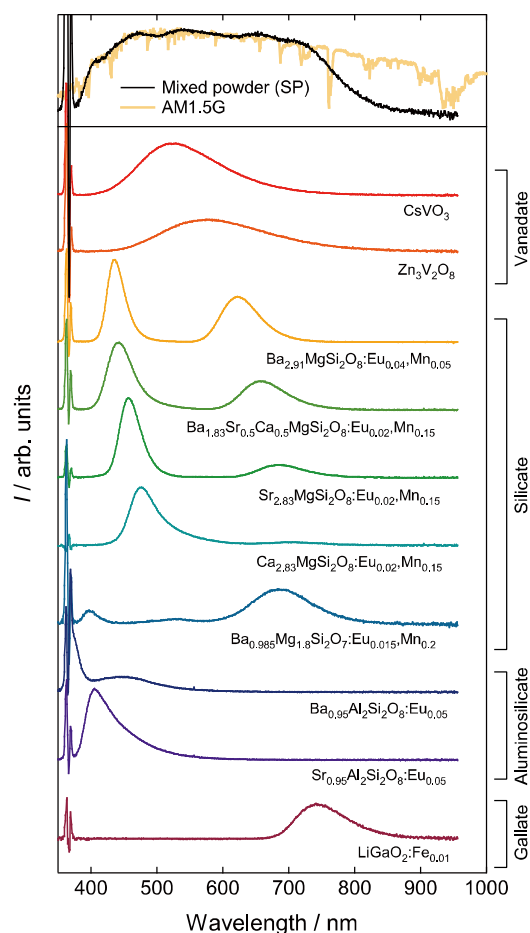
Fig. 3 PL spectra of the vanadates, silicates, aluminosilicates, gallate phosphors, SP, and AM1.5G.

Figure 3 shows the PL spectra for the phosphors and the phosphor mixture. The PL spectrum of the phosphor mixture with the composition shown in Table 1 matched the AM1.5G solar spectrum well. The broad emission from $Zn_3V_2O_8$ centered on 575 nm covered most of the visible light wavelengths. The optimum mixing fraction did not produce a simple sum of the individual phosphor spectra; it strongly depended on the multistep excitation from the luminescence of each phosphor, which had different spectral profiles. There were differences of 10–30 nm in the luminescence peak wavelengths of the phosphors used to compensate for the gaps in the spectrum of the vanadates, thus the simulated sunlight spectrum required every phosphor used. This means a minimum of 10 phosphors are necessary to simulate sunlight in our system. We refer to the optimum phosphor mixture that produced the simulated solar spectrum as solar phosphor (SP). The luminescence properties of SP under monochromatic excitation at 365 nm from a Xe lamp source are shown in Table 2. The IQE remained around 30%, and the CIE color coordinates of (0.329,0.343) were located near pure white (0.33,0.33) with a high color rendering index (R_a) of 99. The correlated color temperature (CCT) showed a typical value for daylight of around 5600 K. Thus, our combination of phosphors produces high-quality simulated solar light.

Table 2. Luminescence properties of the SP.[a]

Property[a]	
IQE	29.2
CIE(x,y)	0.329,0.343
R_a	99
CCT	5645

[a]Data obtained under excitation at 365 nm.
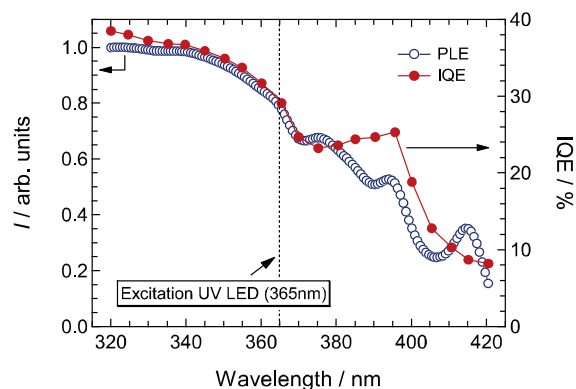
Fig. 4 Wavelength dependence of PLE and IQE for the SP.

Figure 4 shows the wavelength dependence of the PLE and IQE spectra for the SP. The luminescence intensity was saturated below 340 nm, and the IQE reached 36%. The PLE spectrum had a broad band at 320–370 nm related to the charge transfer transition $^1A_1 \rightarrow {}^1T_1, {}^1T_2$ in the VO_4 vanadate tetrahedra,[33] the Eu^{2+} $4f\text{-}5d$ transition, the Mn^{2+} $^6A_1 \rightarrow {}^4T_2$ transition in the silicates and aluminosilicates,[40] and the Fe^{3+} $^6A_1 \rightarrow {}^4T_1$ transition in the gallate.[44] The PLE intensity gradually decreased as the excitation wavelength increased to 370 nm. The spectral shape was complex above 370 nm with some peaks corresponding to the transitions from the $^6A_1$ (^6S) level to the $^4T_2$ (^4D), [$^4A_1$ (^4G), ^4E (^4G)], and $^4T_2$ (^4G) levels of Mn^{2+}.[40,45] Because of the large reduction in the luminescence intensity of vanadate phosphors above 380 nm, excitation at 365 nm was appropriate; however, this indicates the SP emission intensity could be improved if an efficient LED excitation light source with an emission around 350 nm were to be developed.

The red–near-infrared phosphors $Ba_{0.985}Mg_{1.8}Si_2O_7$:$Eu_{0.015}Mn_{0.2}$ and $LiGaO_2$:$Fe_{0.01}$, which formed a large weight fraction of the SP (Table 1), should be optimized more. $Ba_{0.985}Mg_{1.8}Si_2O_7$:$Eu_{0.015}Mn_{0.2}$ emitted deep red light around 700 nm and had a low IQE (26.2%). It formed 11 wt % of the SP, and produced an unexpected absorption and multistep excitation of the Mn^{2+} ions, reducing the overall luminescence intensity. The problem of near-infrared phosphor $LiGaO_2$:$Fe_{0.01}$ was obviously the low absorption (Table 1). Although the IQE of $LiGaO_2$:$Fe_{0.01}$ was relatively high at 76.7%, the external quantum efficiency should be very low because of the low absorption of excitation light. Adding more than 70 wt % of $LiGaO_2$:$Fe_{0.01}$ would scatter the excitation light at the SP plate surface and reduce the efficient absorption of excitation light by other phosphors. Therefore, addressing these problems with red–near-infrared phosphors is the next important step for improving considerably the luminescence properties of the SP.
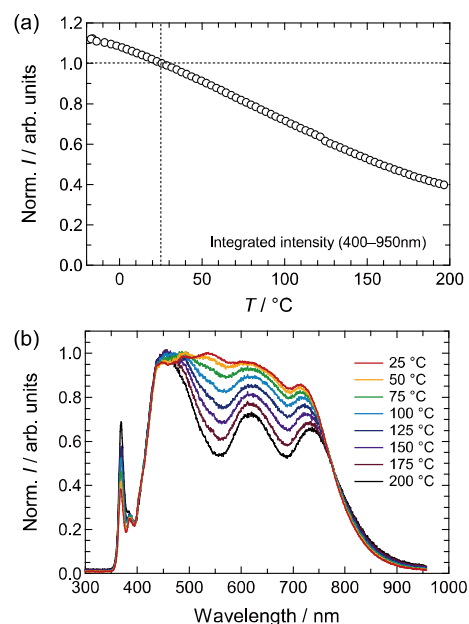
Fig. 5 Temperature dependence of (a) integrated luminescence intensity (400–950 nm) and (b) spectral variation of the SP under excitation at 365 nm.

When the SP was used with a high-power UV LED, the temperature dependence of the luminescence properties became important, due to heat generated by the LED chip. Although the luminescence intensity decreased almost linearly as the temperature increased (Fig. 5a), heating changed the spectral shape dramatically (Fig. 5b). The spectral shape at room temperature (25 °C) remained almost unchanged up to 50 °C, and the luminescence intensity decreased dramatically above 75 °C, particularly around 560 and 680 nm. This indicates that the thermal quenching of the luminescence of $Zn_3V_2O_8$ ($CsVO_3$) and Mn^{2+} in the silicate phosphors, except from $Ba_{2.91}MgSi_2O_8$:$Eu_{0.04}$,$Mn_{0.05}$, was large compared with that of the other phosphors. Therefore, the temperature of the SP in the solar simulator containing a high-power UV LED should be less than 50 °C to maintain the original spectral shape of the simulated sunlight.
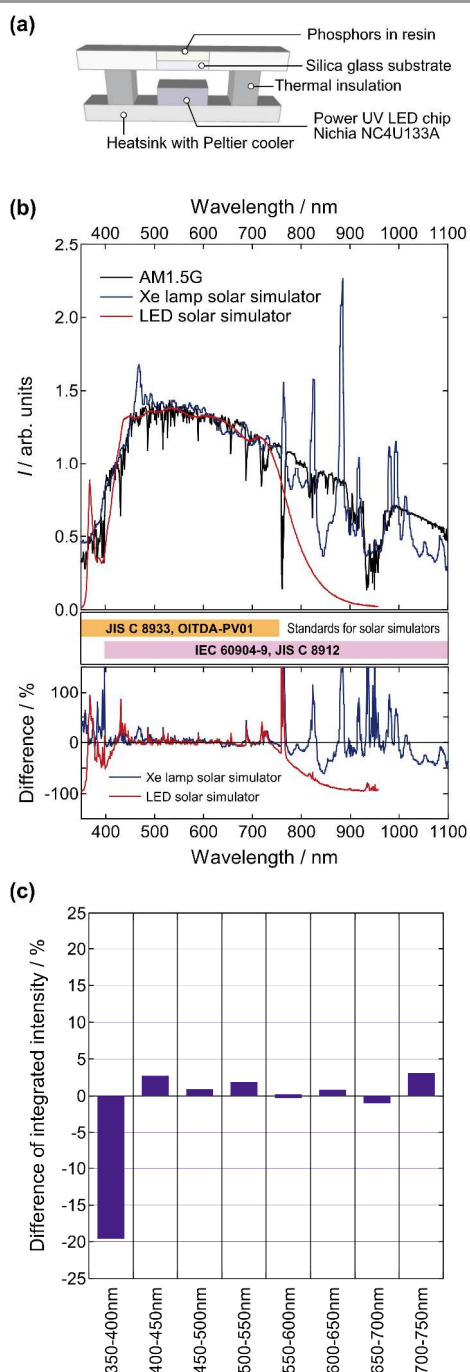
Fig. 6 (a) Schematic of the prototype single-LED solar simulator. (b) The upper panel shows the emission spectra of the LED and conventional Xe lamp solar simulators, and AM1.5G standard spectrum. The corresponding spectral regions for each official solar simulator standard are shown in the middle panel. The bottom panel shows the spectral difference between the standard AM1.5G and solar simulator spectra. (c) The difference between the integrated spectral intensity of the LED solar simulator and AM1.5G for each wavelength region from 350 to 750 nm at intervals of 50 nm.

Fabrication of the single-LED solar simulator and solar cell tests

Figure 6a shows a schematic of the structure of the prototype LED solar simulator consisting of the SP and a high-power UV LED chip with an emission at 365 nm. The SP was not directly embedded in the LED chip as is usually the case,[46] in order to

avoid the thermal degradation of the spectral shape. The SP plate was made by fixing the SP on a silica glass substrate with silicone resin. The SP plate was mounted above the LED chip using a thermally insulating support. The LED chip was attached to a heat sink with a Peltier cooler. When the SP plate was placed directly on the LED chip without the cooling system, the temperature of the SP plate increased above 50 °C.

The emission spectrum of the single-LED solar simulator is shown Fig. 6b. The spectrum successfully reproduced the AM1.5G spectrum in the range of 350–750 nm, which corresponds to the official standards for amorphous Si (JIS C 8933) and dye-sensitized (OITDA-PV01) solar cells. The spectral shape achieved a Class A spectral match with the JIS C 8933 standard.[22] For a Class A match, the difference between the integrated spectral intensity of the solar simulator and AM1.5G in the wavelength regions of 350–400, 400–450, 450–500, 500–550, 550–600, 600–650, 650–700, and 700–750 nm should be kept within ±25%. Figure 5c shows that the difference in the integrated spectral intensity in intervals from 400 to 750 nm was within ±3%, whereas it was still relatively large at −19.6% in the shortest wavelength interval (350–400 nm).

(a)

(b)

(c)
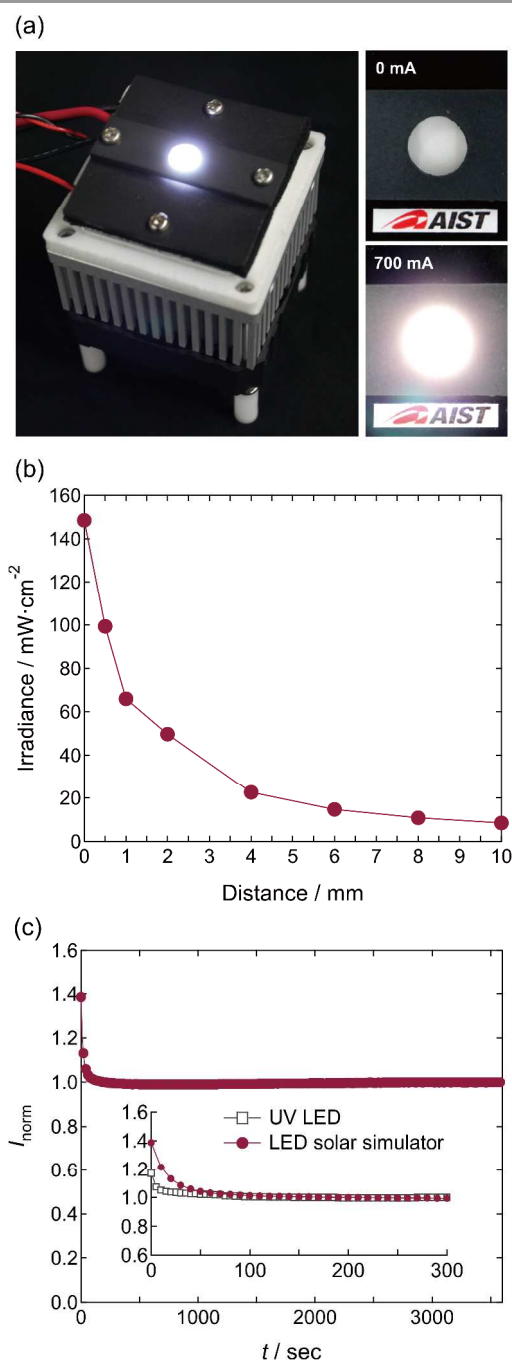
Fig. 7 (a) Photograph of the prototype single-LED solar simulator. The right-hand top and bottom panels show enlarged views of the SP plate at an LED driving current of 0 and 700 mA, respectively. (b) The irradiance at an LED driving current of 700 mA as a function of distance between the top of the LED chip and the bottom of the SP plate. (c) The time dependence of emission light intensity for the LED solar simulator and excitation UV LED.

(a)

(b)
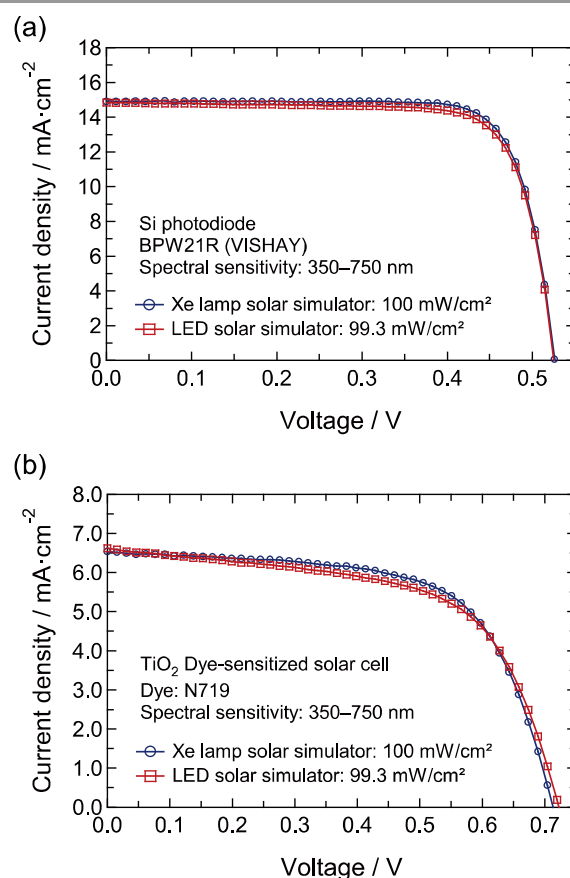
Fig. 8 J-V curves for (a) the Si photodiode and (b) the TiO_2 dye-sensitized solar cell under a Xe lamp and the LED solar simulators at 1 SUN.

Figure 7a shows a photograph of the prototype of the single-LED solar simulator, and the bright simulated sunlight from the SP plate excited from below by a high-power UV LED. This system achieved an irradiance of 100 mW·cm^{-2} (1 SUN) at 0.5 mm with only one LED driven at 11 W (forward current: 700 mA, forward voltage: 15.8 V) (Fig. 7b), while the applicable distance was still close to the light-emitting face at the present stage. But large-scale irradiation at greater distances will be tailored to its application by a larger SP plate and an array of UV LED chips. We strongly suggest that it is exactly a benefit of the SP plate, since the simulated sunlight spectrum is ensured by it. This means the simulated sunlight can be made even in very small devices. Figure 7c shows the stability of the emission light for the LED solar simulator and excitation UV LED source. A light intensity drop was observed in the LED solar simulator immediately after the switching on due to the time variation of excitation UV LED. A slight delay behavior would be originated from the warming SP plate by the radiation heat from the UV LED chip. After 100 s, the LED solar simulator showed very stable emission. The long-range stability of this system would be directly related to the duration of the excitation UV LED chip. Current commercial LED chips have several tens of thousands hour lifetime. Therefore, this point will be a very large advantage of the LED solar simulator compared to conventional Xe lamp solar simulators.

Finally, we compared the performance of our prototype as a solar simulator with that of a conventional Xe lamp system. Figure 8 shows the *J-V* curves for a Si photodiode with the same spectral sensitivity as that of a typical amorphous Si solar cell from 350 to 750 nm, and curves for a TiO_2 dye-sensitized solar cell under 1 SUN illumination. The curves agreed well with each other. The differences in the short-circuit current (I_{sc}) were just 0.36% and 1.37% for the Si photodiode and the TiO_2 dye sensitized solar cell, respectively. The differences in the open-circuit voltage (V_{oc}) were only 0.20% and 1.41% for the Si photodiode and the TiO_2 dye sensitized solar cell, respectively. Thus, our prototype LED solar simulator shows great promise as an efficient alternative for producing simulated sunlight.

Conclusions

We reported a combination of phosphors that simulates the solar spectrum under UV excitation at 365 nm. We used the vanadate phosphors $CsVO_3$ and $Zn_3V_2O_8$, which have intense broadband luminescence, Eu^{2+}/Mn^{2+}-doped silicates and aluminosilicates, and Fe^{2+}-doped Li gallate. The optimized SP had an IQE of 29.2%, an R_a value of 99, and a CCT of 5645 K. We successfully fabricated a prototype LED solar simulator consisting of the SP and a single high-power UV LED. Our simulator achieved a Class A spectral match with the AM1.5G solar spectrum for the JIS C 8933 standard. An irradiance of 100 mW·cm^{-2} (1 SUN) was observed at a forward driving current of 700 mA for the UV LED. The prototype LED solar simulator contained the SP embedded in resin on a silica glass substrate, a high-power UV LED, and a Peltier-cooled heat sink to avoid thermal quenching of the luminescence and variation in the spectral shape. This system functioned well as a solar simulator for actual solar cell testing. The *I-V* curves for a Si photodiode with spectral sensitivity similar to that of an amorphous Si solar cell and for a TiO_2 dye-sensitized solar cell under the LED solar simulator agreed well with the *I-V* curves measured under the conventional Xe lamp solar simulator. Thus, we have demonstrated a potential low-cost, energy-saving solar simulator for solar cell research, which his relevant to huge commercial markets. Moreover, this simple system for emitting high-quality solar light will also be useful for next-generation sunlight lighting systems.

Notes and references

[a] Advanced Manufacturing Research Institute, National Institute of Advanced Industrial Science and Technology, Tsukuba Central 5, 1-1-1 Higashi, Tsukuba, Ibaraki, Japan. Tel: +81-29-861-6368; E-mail: t-nakajima@aist.go.jp

1   A. Goetzberger, C. Hebling and H. W. Schock, *Mater. Sci. Eng. R.*, 2003, **40**, 1.
2   M. A. Green, K. Emery, Y. Hishikawa, W. Warta and E. D. Dunlop, *Prog. Photovolt: Res. Appl.*, 2012, **20**, 12.
3   A. Shah, P. Torres, R. Tscharner, N. Wyrsch and H. Keppner, *Science*, 1999, **285**, 692.
4   M. Grätzel, *Accounts Chem. Res.*, 2009, **42**, 1788.
5   D. Mills, *Sol. Energy*, 2004, **76**, 19.
6   M. Thirugnanasambandam, S. Iniyan and R. Goic, *Renew. Sust. Energ. Rev.*, 2010, **14**, 312.
7   A. Hepbasli, *Renew. Sust. Energ. Rev.*, 2008, **12**, 593.
8   F. E. Osterloh, *Chem. Soc. Rev.*, 2013, **42**, 2294.
9   J. Augustynski, B. D. Alexander and R. Solarska, *Top Curr. Chem.*, 2011, **303**, 1.
10 Z. Li, W. Luo, M. Zhang, J. Feng and Z. Zou, *Energy Environ. Sci.*, 2013, **6**, 347.
11 P. Lianos, *J. Hazard. Mater.*, 2011, **185**, 575.
12 T. Kozai, *Proc. Jpn. Acad., Ser. B*, 2013, **89**, 447.
13 K. Kato, R. Yoshida, A. Kikuzaki, T. Hirai, H. Kuroda, K. Hiwasa-Tanabe, K. Takane, H. Ezura and T. Mizoguchi, *J. Agric. Food Chem.*, 2010, **58**, 9505.
14 N. Yeh and J-P. Chung, *Renew. Sust. Energ. Rev.*, 2009, **13**, 2175.
15 R. M. Sayre, C. Cole, W. Billhimer, J. Stanfield and R. D. Ley, *Photodermatol. Photoimmunol. Photomed.*, 1990, **7**, 159.
16 K. A. Emery, *Solar Cells*, 1986, **18**, 251.
17 R. M. Sayre, J. Stanfield, A. J. Bush and D. L. Lott, *Photodermatol. Photoimmunol. Photomed.*, 2001, **17**, 278.
18 ASTM G173-03(2012): *Standard tables for reference solar spectral irradiances: Direct normal and hemispherical on 37° tilted surface.*
19 S. P. Bremner, M. Y. Levy and C. B. Honsberg, *Prog. Photovolt: Res. Appl.*, 2008, **16**, 225.
20 IEC 60904-9-Ed. 2: *Photovoltaic devices – Part 9: Solar simulator performance requirements.*
21 JIS C 8912: 2011: *Solar simulators for crystalline solar cells and modules.*
22 JIS C 8933: 2011: *Solar simulators for amorphous solar cells and modules.*
23 OITDA-PV01-2009: *Evaluation method of performance for dye-sensitized solar devices.*
24 A. Nakajima, M. Ichikawa, T. Sawada, M. Yoshimi and K. Yamamoto, *Jpn. J. Appl. Phys.*, 2004, **43**, 7296.
25 S. Kohraku and K. Kurokawa, *Sol. Energy Mater. Sol. Cells*, 2006, **90**, 3364.
26 D. Kolberg, F. Schubert, K. Klameth and D. M. Spinner, *Energy Procedia*, 2012, **27**, 306.
27 A. Namin, C. Jivacate, D. Chenvidhya, K. Kirtikara and J. Thongpron, *Renew. Energy*, 2013, **54**, 131.
28 M. Bliss, T. R. Betts and R. Gottshalg, *Sol. Energy Mater. Sol. Cells*, 2009, **93**, 825.
29 S. H. Jang and M. W. Shin, *Curr. Appl. Phys.*, 2010, **10**, S537.
30 B. H. Hamadani, K. Chua, J. Roller, M. J. Bennahmias, B. Campbell and H. W. Yoon, *Prog. Photovolt: Res. Appl.*, 2013, **21**, 779.
31 H. Gobrecht and G. Heinsohn, *Z. Phys.*, 1957, **147**, 350.
32 T. Nakajima, M. Isobe, T. Tsuchiya, Y. Ueda and T. Kumagai, *Nat. Mater.*, 2008, **7**, 735.
33 T. Nakajima, M. Isobe, T. Tsuchiya, Y. Ueda and T. Manabe, *J. Phys. Chem. C*, 2010, **114**, 5160.
34 T. Nakajima, M. Isobe, T. Tsuchiya, Y. Ueda and T. Kumagai, *J. Lumin*, 2009, **129**, 1598.
35 T. Nakajima, M. Isobe, T. Tsuchiya, Y. Ueda and T. Manabe, *Opt. Mater.*, 2010, **32**, 1618.
36 K. Tadatomo, H. Okagawa, Y. Ohuchi, T. Ysunekawa, Y. Imada, M. Kato and T. Taguchi, *Jpn. J. Appl. Phys.*, 2001, **40**, L583.
37 D. Morita, M. Yamamoto, K. Akaishi, K. Matoba, K. Yasutomo, Y. Kasai, M. Sato, S. Nagahama and T. Mukai, *Jpn. J. Appl. Phys.*, 2004, **43**, 5945.
38 T. L. Barry, *J. Electrochem. Soc.*, 1968, **115**, 733.
39 S. Ye, J. Zhang, X. Zhang, S. Lu, X. Ren and X. Wang, *J. Appl. Phys.*, 2007, **101**, 033513.
40 L. Ma, D-J. Wang, Z-Y. Mao, Q-F. Lu and Z-H. Yuan, *Appl. Phys. Lett.*, 2008, **93**, 144101.
41 K. Sinha, B. Pearson, S. R. Casolco, J. E. Garay and O. A. Graeve, *J. Am. Ceram. Soc.*, 2009, **92**, 2504.
42 J. G. Rabatin, *J. Electrochem. Soc.*, 1978, **125**, 920.
43 B. O'Regan and M. Grätzel, *Nature*, 1991, **353**, 737.
44 R. Heitz, A. Hoffmann and I. Broser, *Phys. Rev. B*, 1992, **45**, 8977.

45 C-H. Huang, T-W. Kuo and T-M. Chen, *ACS Appl. Mater. Interfaces*, 2010, **2**, 1395.
46 P. Schlotter, R. Schmidt and J. Schneider, *Appl. Phys. A*, 1997, **64**, 417.
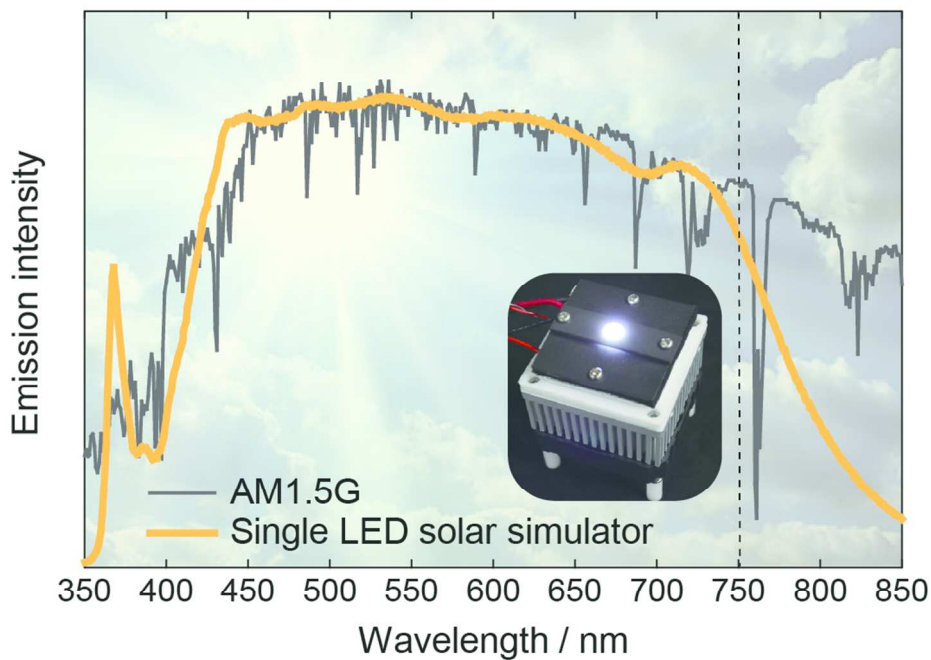
Smallest sun: single LED solar simulator that shows high quality simulated solar spectrum in accordance with the AM1.5G standard has been developed.
98x69mm (300 x 300 DPI)